

Sorting of Two Polytopic Proteins, the γ -Aminobutyric Acid and Betaine Transporters, in Polarized Epithelial Cells*

(Received for publication, June 25, 1996, and in revised form, October 28, 1996)

Carla Perego[‡], Alessandra Bulbarelli[‡], Renato Longhi[§], Marco Caimi[¶], Antonello Villa[¶], Michael J. Caplan^{||}, and Grazia Pietrini^{‡**}

From the [‡]Consiglio Nazionale delle Ricerche Cellular and Molecular Pharmacology Center, Department of Pharmacology, University of Milan, Milan 20129, the [§]Consiglio Nazionale delle Ricerche Institute of Hormone Chemistry, Milan 20129, the [¶]DIBIT-San Raffaele Scientific Institute and Ceccarelli Center, Milan 20132, Italy, and the ^{||}Department of Cellular and Molecular Physiology, Yale University School of Medicine, New Haven, Connecticut 06510

The γ -aminobutyric acid transporter (GAT-1) isoform of the γ -aminobutyric acid and the betaine (BGT) transporters exhibit distinct apical and basolateral distributions when introduced into Madin-Darby canine kidney cells (Pietrini, G., Suh, Y. J., Edelman, L., Rudnick, G., and Caplan, M. J. (1994) *J. Biol. Chem.* 269, 4668–4674). We have investigated the presence of sorting signals in their COOH-terminal cytosolic domains by expression in Madin-Darby canine kidney cells of mutated and chimeric transporters. Whereas truncated GAT-1 (Δ C-GAT) maintained the original functional activity and apical localization, either the removal (Δ C-myc BGT) or the substitution (BGS chimera) of the cytosolic tail of BGT generated proteins that accumulated in the endoplasmic reticulum. Moreover, we have found that the cytosolic tail of BGT redirected apical proteins, the polytopic GAT-1 (GBS chimera) and the monotopic human nerve growth factor receptor, to the basolateral surface. These results suggest the presence of basolateral sorting information in the cytosolic tail of BGT. We have further shown that information necessary for the exit of BGT from the endoplasmic reticulum and for the basolateral localization of the GBS chimera is contained in a short segment, rich in basic residues, within the cytosolic tail of BGT.

The plasma membranes of polarized epithelial cells are divided into apical and basolateral domains that are characterized by distinct lipid and protein compositions. The generation and maintenance of the polarized distribution of surface proteins require sorting of newly synthesized membrane proteins to their appropriate sites of residence. Thus, although the molecular mechanisms are still poorly understood, membrane proteins located apically and basolaterally must contain sorting determinants recognized by the cellular sorting machinery.

So far, the search for apical and basolateral sorting determinants has been largely focused on monotopic proteins (for review, see Ref. 2). Two classes of basolateral sorting determinants have been identified: one related to coated pit localization, and in most cases relying on the same tyrosine residue required for endocytosis (3–7); the other unrelated to

endocytosis signals (5, 8, 9). Despite their heterogeneity, all of the identified basolateral sorting determinants have been found to be located in the cytosolic domains of basolaterally expressed plasma membrane proteins.

Whereas the identification of two classes of basolateral sorting signals formally demonstrates that the basolateral pathway is signal-mediated, the lack of identified apical sorting signals in transmembrane proteins leaves open the question of whether the apical pathway occurs by default or by a signal-mediated mechanism. In favor of a signal-mediated pathway is the observation that glycoposphatidylinositol-anchored proteins are predominantly localized on the apical surface of MDCK¹ cells (10, 11) and that their glycoposphatidylinositol anchors function as apical sorting signals (12, 13). In addition, *N*-glycosylation has been shown to be involved in the apical targeting of a secretory protein and has been proposed to function as apical sorting signal of transmembrane proteins as well (14). On the other hand, the removal of a basolateral sorting signal from a basolaterally targeted protein can lead to its preferential appearance on the opposite apical domain (5, 7, 8, 15), suggesting that apical sorting could occur by default or that a hierarchy of signals may occur, with the basolateral signal in the cytoplasmic domain operating as dominant over the weaker apical signal located in the luminal domain (2).

Sorting signals responsible for apical and basolateral delivery of polytopic proteins have only recently begun to be investigated (16, 17). We wondered if monotopic and polytopic proteins exploit similar signals and mechanisms to reach their cellular destination. In particular, we were interested in clarifying whether basolateral sorting signals of polytopic proteins are located in their cytoplasmic tails and whether they might cause the basolateral relocation of apical proteins.

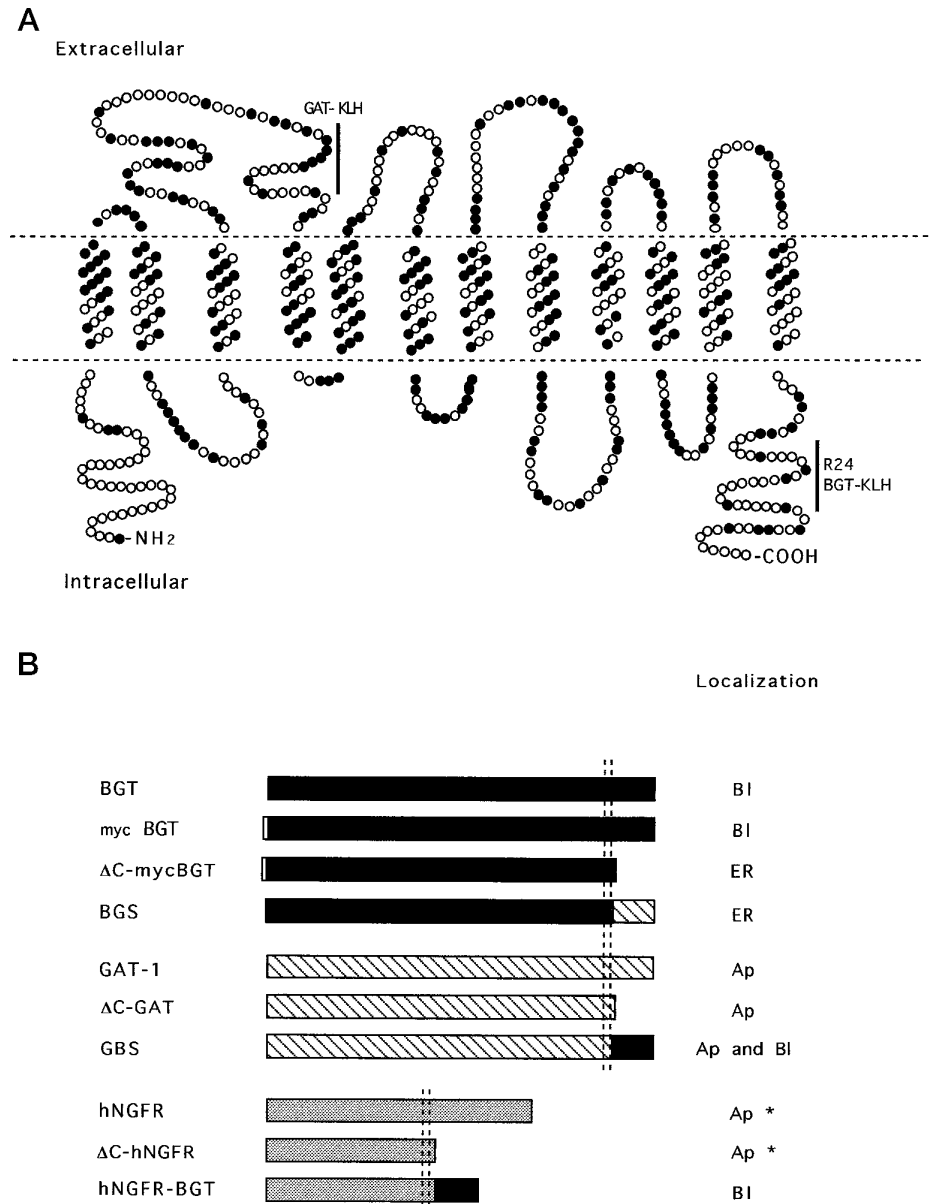
To study sorting determinants of polytopic proteins, we have used as models two related transporter proteins: the GAT-1 isoform of the γ -aminobutyric acid (GABA) transporter (18) and the dog betaine transporter (BGT) (19). These proteins contain 12 putative hydrophobic transmembrane α -helices, with both amino and carboxyl termini predicted to face the cytoplasm (see Fig. 1A). GAT-1 and BGT are members of the same sodium- and chloride-dependent neurotransmitter transporter gene family, share high structural (60% of identity at the amino acid level, see Fig. 1A) and functional (they both transport GABA) similarities, and both exert their specific function in polarized cells (20). Whereas GAT-1 is expressed predominantly on ax-

* This work was supported in part by Consiglio Nazionale delle Ricerche Grant 94.00377.CT14.115.28212B/0004 (to G. P.). The costs of publication of this article were defrayed in part by the payment of page charges. This article must therefore be hereby marked "advertisement" in accordance with 18 U.S.C. Section 1734 solely to indicate this fact.

** To whom correspondence should be addressed: CNR Cellular and Molecular Pharmacology Center, Via Vanvitelli, 32, 20129 Milano, Italy. Tel.: 39-2-701-46358; Fax: 39-2-749-0574; E-mail: Grazia@Farma1.csfc.mi.cnr.it.

¹ The abbreviations used are: MDCK, Madin-Darby canine kidney; GABA, γ -aminobutyric acid; GAT-1, GABA transporter; BGT, betaine transporter; hNGFR, human nerve growth factor receptor; PCR, polymerase chain reaction; KLH, keyhole limpet hemocyanin; ER, endoplasmic reticulum; mAb, monoclonal antibody.

FIG. 1. Structure of GAT-1 and BGT and representation of mutants and chimeras used in this study with their localization in transfected MDCK cells. Panel A, predicted transmembrane topology of betaine and GABA transporters. Filled circles represent amino acids that are identical in BGT and GAT-1. Positions of synthetic peptides used to raise the indicated antibodies are shown. Panel B, wild type and truncated transporters, as well as the chimeras constructed in this study are shown schematically, and their localization in transfected MDCK cells is indicated. The contributions of BGT (filled bars), GAT-1 (hatched bars), and hNGFR (dotted bars) cDNAs are indicated in each chimera. The location of the Myc tag is indicated by the white bar at the NH₂ terminus of BGT. The Myc sequence in myc BGT and ΔC-myc BGT was inserted immediately after the AUG start codon. The last 49 amino acids at the COOH terminus of BGT were deleted in the ΔC-myc BGT construct. The COOH termini of GAT-1 and BGT were exchanged from the first amino acid after transmembrane 12 in the BGS and GBS chimeras. ΔC-GAT was constructed by removal of the last 36 amino acids of GAT-1. The cytosolic tail of hNGFR was replaced by 51 amino acids of the cytosolic tail of BGT. The vertical dashed double line indicates the 12th transmembrane domain of the transporters and the unique transmembrane domain of hNGFR. * The apical localizations of hNGFR and ΔC-hNGFR have been established in previous studies by Le Bivic *et al.* (4).



onal processes of GABA-ergic neurons (1, 21) where it mediates GABA reuptake, BGT is accumulated on the basolateral domain of renal epithelial cells exposed to hyperosmotic conditions (22). We have shown previously that GAT-1 and BGT localize to opposite plasma membrane domains when transfected in MDCK cells (1). Thus, these two homologous proteins provide a good system for the investigation of apical and basolateral sorting determinants in polytopic proteins. Our results show that, as is true for monotopic basolateral proteins, BGT contains a basolateral sorting determinant in a cytosolic domain. In addition, they suggest the presence of strong apical determinants in GAT-1.

EXPERIMENTAL PROCEDURES
Plasmid Constructions

The original BGT and GAT-1 clones were kindly provided by J. S. Handler (Johns Hopkins University) and B. Kanner (Hebrew University) and were subcloned in the mammalian expression vector pCB6 (1). Wild type hNGFR cDNA (23) subcloned into *EcoRI-BamHI* restriction sites of pCB6 was kindly provided by A. Le Bivic (D'Aix-Marseille II University, CNRS UMR 9943). To generate mutants and chimeras, PCR amplifications were performed, and the PCR products were cloned into pCB6. The absence of unwanted substitutions in the mutant clones,

due to the amplification processes, was checked by sequencing. The sequences of all primers are available on request. A representation of the mutants and chimeras is given in Fig. 1B.

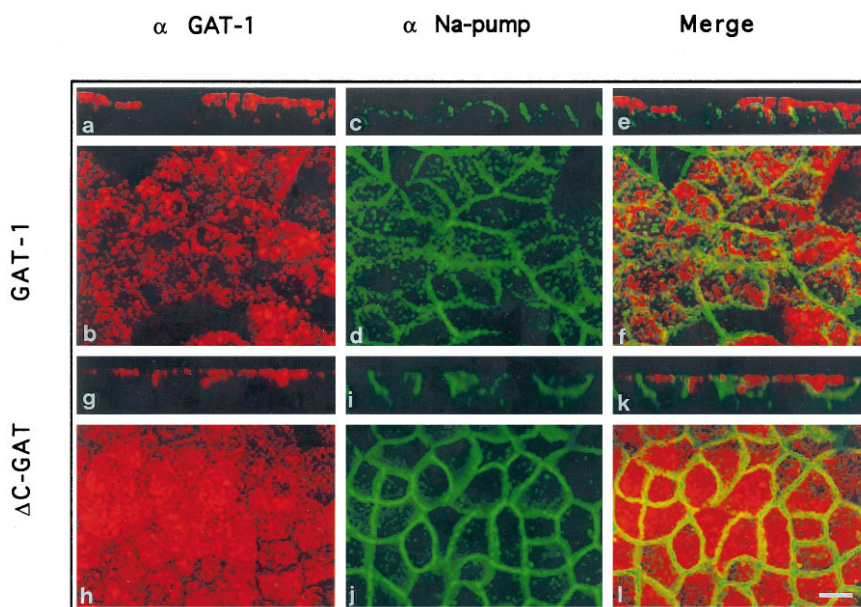
ΔC-GAT (Tail-minus GAT-1)—The last COOH-terminal 36 amino acids of GAT-1 were removed. This mutant was generated by PCR amplification using GAT-1 cDNA as template. A T was inserted to change the codon Lys in position 564 of the wild type GAT-1 to a TAA stop codon. The *SmaI-XbaI* fragment of pCB6-GAT-1 was replaced with the similarly digested PCR product.

Myc BGT—The sequence of the c-Myc epitope tag EQKLISEEDL was inserted just after the ATG codon corresponding to the first methionine in BGT cDNA by PCR amplification. The PCR product was digested with *MluI-EcoRI* and ligated into similarly digested pCB6-BGT.

ΔC-myc BGT (Tail-minus BGT)—The last COOH-terminal 49 amino acids were removed from the cDNA encoding myc BGT. A fragment containing an in-frame stop codon was originated by insertion of a T in position 1814 of BGT in a PCR using BGT as template. The PCR product was digested with *SmaI-ClaI* and ligated into similarly digested pCB6-myc BGT.

BGS Chimera—The last COOH-terminal 56 amino acids of BGT were replaced with the analogous 43 amino acids of GAT-1 by two rounds of sequential PCR amplification. Two separate reactions were carried out. In the first round, reaction 1, BGT cDNA was used as template with primers 1a (corresponding to nucleotides 1352–1378 of the BGT sequence) and 1b (containing 21 nucleotides complementary to

FIG. 2. Immunofluorescence analysis of the surface distribution of GAT-1 and Δ C-GAT in transfected MDCK cells. GAT-1 (panels a–f) and Δ C-GAT (panels g–l) transfected MDCK cells grown to confluence on Transwell filters were fixed with ice-cold methanol and double stained with anti-GAT-1 R24 (panels a and b) or GAT-KLH (panels g and h) antibodies (in red) and with mAb 6H against the sodium pump (panels c, d, i, and j) (in green). Confocal immunofluorescence micrographs of vertical (panels a, c, e, g, i, and k) or horizontal (panels b, d, f, h, j, and l) focal planes are shown. Note that horizontal sections were taken at a focal plane which include portions of both the apical and basolateral surfaces. A merge of the two patterns (panels e, f, k, and l) clearly shows a lack of colocalization of GAT-1 and Δ C-GAT with the basolateral marker sodium pump. Bar, 15 μ m.



oligonucleotide Ic, followed by 21 nucleotides complementary to nucleotides 1792–1772 of BGT). In reaction 2, GAT-1 was used as template with primers Ic (corresponding to nucleotides 1860–1880 of GAT-1) and Id (complementary to bases 1000–983 of the pCB6 cloning vector, containing the *Xba*I restriction site). In the second round of amplification the products of the first round of PCR were used as template and oligonucleotides Ia and Id as primers. The fusion product was generated by virtue of the 21-nucleotide overlap between the fragments generated in the first round. The *Acc*III-*Xba*I digest of this PCR product was ligated into similarly digested pCB6-BGT.

GBS Chimera—The last COOH-terminal 43 amino acids of GAT-1 were replaced with the analogous 56 amino acids of BGT. A fragment containing the cDNA coding for the COOH-terminal 56 amino acids of BGT was generated using BGT as template and as upper primer an oligonucleotide corresponding to nucleotides 1836–1859 of the GAT-1 sequence fused to 1793–1822 of BGT; a T was changed from a C in position 1801 of the BGT sequence to eliminate the *Sma*I site. The lower primer was complementary to the 3′-noncoding region of BGT and contained a *Cla*I restriction site. The PCR fragment was digested with *Sma*I and *Cla*I restriction enzymes and ligated to similarly digested pCB6-GAT-1.

hNGFR-BGT Chimera—The COOH-terminal 51 amino acids of BGT were fused to amino acid 278 of p75 hNGFR cDNA to generate a recombinant receptor with the cytoplasmic tail replaced with that of BGT. A PCR was carried out using BGT as template. The sequences of the upper primer contained a *Pvu*II site in its 5′ extremity. The PCR fragment was digested with *Pvu*II and *Cla*I and ligated into similarly digested pCB6-hNGFR.

BGT Δ 565–572—A deletion of amino acids 565–572 (see Fig. 7A) in the COOH terminus of BGT was introduced by PCR amplification using BGT as template and an oligonucleotide corresponding to bases 1799–1813 fused to 1835–1843 of BGT as upper primer. The lower primer was as for the GBS chimera. The *Sma*I-*Cla*I fragment of pCB6-BGT was replaced with similarly digested PCR product.

GBS Δ 565–572—The last COOH-terminal 43 amino acids of GAT-1 were replaced with the analogous 48 amino acids of BGT Δ 565–572 by PCR amplification using as upper primer an oligonucleotide corresponding to nucleotides 1836–1859 of the GAT-1 sequence fused to 1793–1849 of the BGT sequence in which nucleotides 1810–1835 were removed and GBS as template. The lower primer was as for the GBS chimera. The *Sma*I-*Cla*I fragment of pCB6-GBS was replaced with the similarly digested PCR product.

Cell Culture and Transfection

MDCK (strain II) cells were grown and transfected with the calcium phosphate method as described previously (1). Transfected cell lines were selected by growth in the antibiotic G418 (0.9 mg/ml) (Life Technologies, Inc.). Expression of recombinant proteins was assayed initially by GABA uptake and/or by immunofluorescence. At least three independent clones were analyzed for each recombinant cell line, and similar polarity ratios were observed. For all polarity studies trans-

fecting and untransfected MDCK cells were grown to confluence for more than 5 days on 0.4- μ m pore size Transwell filter inserts (Costar).

Antibodies and Immunocytochemistry

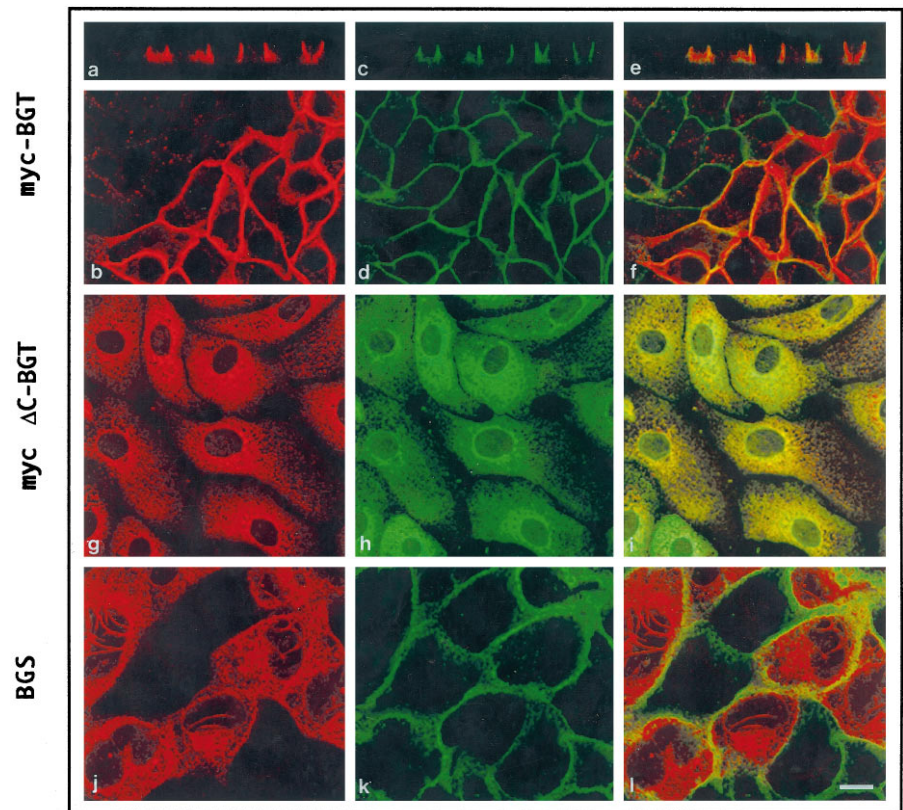
To localize wild type and chimeric transporters in both immunofluorescence and immunoprecipitation experiments the following antibodies were used. GAT-1 and the BGS chimera were localized with antibody R24, kindly provided by R. Jahn (Yale University). The antibody was generated against a synthetic peptide corresponding to amino acids 571–586 in the COOH-terminal domain of GAT-1 (see Fig. 1A). Coupling and immunization were performed as described (1). To localize Δ C-GAT we used a rabbit polyclonal serum (GAT-KLH) (keyhole limpet hemocyanin) produced against a synthetic peptide comprising amino acids 189–205 of GAT-1 (in the second extracellular loop, see Fig. 1A). BGT and GBS chimera localization was revealed with an antibody (BGT-KLH) raised against the synthetic peptide comprising amino acids 563–591 in the COOH terminus of BGT (see Fig. 1A). A cysteine followed by a glycine were added at the amino termini of the GAT-KLH and BGT-KLH synthetic peptides to facilitate coupling to KLH. Haptenization to KLH and injection were as described (24, 25). C-Myc epitope-tagged wild type and truncated BGT were localized with clone 9 E10 monoclonal antibody (Oncogene Science). The Na,K-ATPase α 1 subunit was localized using monoclonal antibody 6H. Production and characterization of the 6H antibody are described elsewhere (26). The wild type hNGFR and the chimera hNGFR-BGT were localized using ME 20.4 (kindly provided by A. Le Bivic; 27). An anti-rat ER antibody (28), a gift of D. Louvard, was used in double labeling experiments.

MDCK cells were fixed in ice-cold methanol and processed for immunofluorescence as described previously (29). Wild type and chimeric hNGFR-transfected cells were fixed with freshly made 3% paraformaldehyde in 125 mM sodium phosphate, pH 7.4, for 15 min, and antibody staining was performed with the same protocol but without detergent in the reaction buffer. Fluorescein isothiocyanate-conjugated anti-mouse/rabbit IgG from Jackson ImmunoResearch (West Grove, PA), biotin anti-rabbit/mouse IgG, and Texas red-conjugated streptavidin (Sigma) were used as secondary reagents. Confocal images were obtained using a Bio-Rad MRC-1024 confocal microscope. Micrographs were taken using either a Focus Imagecorder Plus (Focus Graphics Inc.) on Kodak film or a Professional Color Point 2 dye sublimation printer (Seiko).

Steady-state Cell Surface Biotinylation

Confluent cells grown on 24-mm Transwell filters were starved for 30 min in Dulbecco's modified Eagle's medium without cysteine and methionine and metabolically labeled overnight with 0.1 mCi/ml Tran³⁵S-label (ICN Pharmaceuticals, Costa Mesa, CA) (30). Biotinylation with NHS-ss-biotin (Pierce Chemical Co.) on the apical or basolateral side was performed according to Sargiacomo *et al.* (31). Following biotinylation cells were lysed, and the protein of interest was incubated with the primary antibodies described in the preceding section. Following the primary incubation, anti-rabbit/mouse IgG-conjugated agarose (Sigma) secondary antibodies were added. Transporters were released from the

FIG. 3. Immunofluorescence analysis of the cellular distribution of wild type, truncated, and chimeric BGT in transfected MDCK cells. Confluent MDCK cells transfected with Myc-tagged BGT (panels *a-f*), Myc-tagged Δ C-BGT (panels *g-i*), or BGS chimera (panels *j-l*) were stained with the polyclonal BGT-KLH raised against BGT (panels *a* and *b*), anti-Myc epitope mAb 9E10 (panel *g*), or polyclonal R24 against the cytosolic tail of GAT-1 (panel *j*) antibodies (in red), and double stained with anti-sodium pump mAb 6H (panels *c*, *d*, and *k*) or polyclonal anti-ER (panel *h*) antibodies (in green). Confocal immunofluorescence micrographs of vertical (panels *a* and *c*) or horizontal (panels *b*, *d*, *g*, *h*, *j*, and *k*) focal planes and merging of the two staining patterns are shown (panels *e*, *f*, *i*, *l*). Yellow/orange colors indicate colocalization. The addition of the c-Myc epitope in the NH₂ terminus of BGT does not interfere with the basolateral localization of the transporter, whereas removal or substitution of the cytosolic tail of BGT generates proteins unable to reach the cell surface. Bar, 15 μ m.



beads by boiling in 10 μ l of 10% SDS, and surface-biotinylated transporters were reprecipitated with streptavidin beads (Pierce). The beads were then heated in SDS solubilization buffer, and the released reduced proteins were alkylated and analyzed on 10% SDS-polyacrylamide gel electrophoresis (32). Quantitation of the biotinylated proteins was performed by scanning the developed fluorograph with a LKB Ultrascan XL laser densitometer.

GABA Influx Assay

GABA influx was performed according to Yamauchi *et al.* (22) with modifications (1). Cells were washed twice with incubation buffer (150 mM NaCl, 2 mM KCl, 1 mM CaCl₂, 1 mM MgCl₂, 10 mM HEPES, pH 7.5) and incubated in the same solution containing [³H]GABA (DuPont NEN). Briefly, for screening for stable transfectants, cells grown on 24-well plates were incubated in 0.2 ml of incubation buffer containing 0.5 μ Ci of [³H]GABA for 10 or 30 min to measure GAT-1 or BGT activity, respectively. To study the polarity of expressed transporters the cells were grown to confluent density for 7 days on 6.5-mm Transwell filters. [³H]GABA in incubation buffer was applied either on the apical (100 μ l) or basolateral (250 μ l) side at a final concentration of 10 μ M for 10 min (for wild type GAT-1 and related mutants) or 100 μ M for 30 min (for wild type BGT and related mutants). Uptake was terminated by aspirating the medium, and the cells were washed three times with ice-cold incubation buffer. After cell solubilization in 0.2 ml of 1% SDS (when filters were used they were removed from the supports before cell solubilization) the samples were counted in 5 ml of scintillation solution (Ultima Gold, Packard).

RESULTS

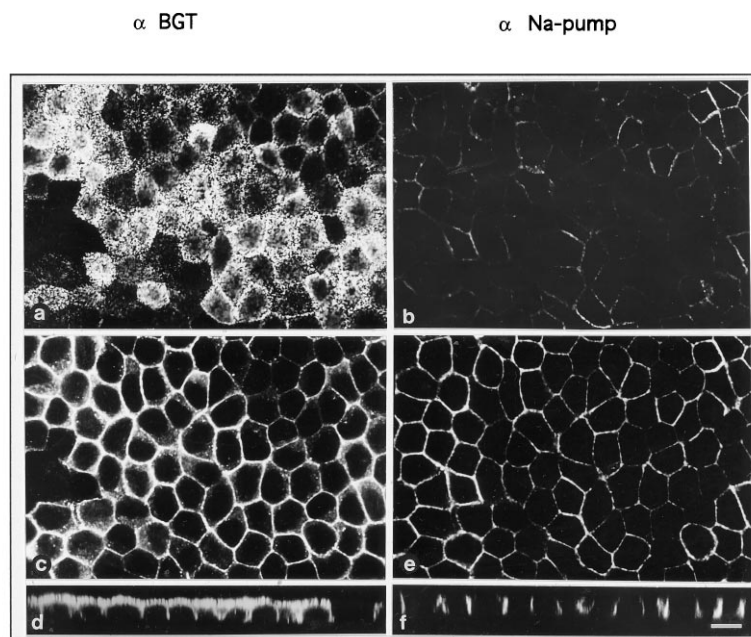
Previous results obtained in our laboratory indicate that the neuronal GAT-1 and the epithelial BGT, despite their high structural (Fig. 1A) and functional similarity, bear opposite apical and basolateral sorting signals. Indeed, stably transfected MDCK cells localize GAT-1 and BGT apically and basolaterally, as shown previously (1) and in Figs. 2 and 3, *a-f*, of this paper. Therefore, we first tested for the presence of apical and basolateral sorting signals in the COOH-terminal domain of GAT-1 and BGT, which is a domain with a low degree of similarity between the two proteins. For this purpose we generated, by recombinant DNA technology, truncated and chi-

meric transporters (schematically represented in Fig. 1 and described under "Experimental Procedures"), and their sorting behavior was analyzed in MDCK cells.

The COOH-terminal 36 Amino Acids of GAT-1 Are Not Required for the Protein's Functional Activity and Apical Localization—The distribution of the wild type and truncated GAT-1 (Δ C-GAT) stably expressed in MDCK cells was investigated by double immunostaining with the antipeptide antibodies raised against GAT-1 (Fig. 2, in red) and the basolateral marker α 1 subunit of the sodium pump (Fig. 2, in green). Horizontal (XY section) and vertical (XZ cross-section) images were obtained by confocal laser scanning analysis. A punctate pattern, typical of apical microvillar staining, was revealed by the GAT-1 antibodies in horizontal sections both in MDCK cells expressing the wild type (*b* and *f*) and the truncated transporters (*h* and *l*). The predominant apical localization of GAT-1 and Δ C-GAT is clearly identifiable in vertical sections (compare Fig. 2, *a* and *g* with *c* and *i*, respectively). Virtually no yellow color, indicating colocalization with the basolateral marker, was revealed by merging of the confocal images. These data show that the removal of the last 36 amino acids in the wild type GAT-1 does not affect the apical localization of the protein. Together with the unaltered sorting behavior, the deleted GAT-1 transporter retained its functional surface activity, as shown by the GABA uptake assay (see Fig. 5C).

Information for Exit from the ER Is Contained within the COOH-terminal Domain of BGT—The cellular distribution of wild type and tail-minus BGT was followed by indirect immunofluorescence microscopy. To allow the localization of the truncated BGT a c-Myc epitope was inserted at the amino-terminal domain of the transporter. In Fig. 3, *a-f*, epitope-tagged BGT-transfected MDCK cells were double stained with BGT-KLH (in red) and with mAb 6H (in green) antibodies. Colocalization of the tagged BGT with the basolateral marker is revealed by comparison of the confocal analysis. The yellow/orange color in the merge of vertical and horizontal sections (*e*

FIG. 4. Immunofluorescence analysis of the surface distribution of the GBS chimera in transfected MDCK cells. Cells grown to confluent density on Transwell filters after ice-cold methanol fixation were double stained with polyclonal BGT-KLH (panels *a*, *c*, and *d*) and mAb 6H against the sodium pump (panels *b*, *e*, and *f*) antibodies. Confocal immunofluorescence micrographs of horizontal sections through the apical (panels *a* and *b*) and the basal (panels *c* and *e*) surface of the monolayer, and vertical focal planes (panels *d* and *f*) are shown. The apical and basolateral localization of the GBS chimera demonstrates the presence in the BGT tail of a basolateral sorting signal. Bar, 15 μm .



and *f*) furthermore demonstrate colocalization of the two antigens. A similar distribution of the tagged BGT was observed using the antibody against the Myc epitope. No specific staining with the BGT antibody was observed in untransfected MDCK cells (as shown in *b*, where nonexpressing cells devoid of staining are observed). This was not surprising in light of a low endogenous expression of BGT in MDCK cells grown in isotonic medium, as demonstrated previously (1, 22).

The unchanged basolateral localization of the tagged BGT allowed us to analyze the sorting behavior of the deleted epitope-tagged BGT ($\Delta\text{C-myc BGT}$). Immunolocalization experiments carried out in $\Delta\text{C-myc BGT}$ -transfected MDCK cells showed an intracellular distribution of the tailless BGT typical of ER localization (Fig. 3*g*). No staining was observed in untransfected MDCK cells with the antibody raised against the Myc epitope (data not shown). Double staining with an antibody raised against an ER marker (28) confirmed the ER localization of the truncated BGT (revealed by the yellow staining, *i*). The inability of the truncated transporter to reach the cell surface was further confirmed by the [^3H]GABA uptake transport assay. No surface transport activity was observed, even after enhancing the expression of exogenous proteins by overnight treatment with 10 mM sodium butyrate (33) (data not shown).

Consensus sequences for ER retrieval have been identified in the extremity of cytoplasmic carboxyl termini of ER resident membrane proteins (34). To exclude that an internal potential ER retrieval motif was unmasked by the removal of the COOH-terminal 49 amino acids in the epitope-tagged $\Delta\text{C-myc BGT}$, the BGT tail was replaced by the GAT-1 tail. The inability of the GAT-1 tail to restore the surface expression of BGT was revealed by confocal microscope analysis of transfected MDCK cells (*j-l*) and by [^3H]GABA transport experiments (data not shown). These data suggest that information necessary for the BGT exit from the ER is contained in the cytosolic tail of BGT.

Basolateral Sorting Information Is Contained within the Cytosolic COOH-terminal 51 Amino Acids of BGT—The ER accumulation of truncated BGT prevented the determination of a possible involvement of the cytosolic tail in the specific basolateral localization of the transporter. Therefore, we generated a GABA transporter chimera containing the BGT tail (GBS, see Fig. 1). The cellular distribution of GBS was detected by indirect double immunofluorescence. Confocal images generated at

the horizontal focal plane of the apical surface of GBS-transfected MDCK cells revealed apical localization of the chimera (compare Fig. 4, *a* and *b*). However, in contrast to the situation with the wild type GAT-1, the chimera was also found on the basolateral surface as displayed by the horizontal section obtained at the basal focal plane, as well as by the vertical section (compare *c* and *d* with *e* and *f*).

The apical to basolateral polarity ratio of wild type and mutant transporters was determined by cell surface biotinylation experiments and influx studies (Fig. 5).

The steady-state biotinylation experiment (Fig. 5*A*) demonstrated that whereas GAT-1 and $\Delta\text{C-GAT}$ are available to cell surface biotinylation predominantly from the apical side, BGT is predominantly biotinylated when the NHS-biotin was added to the basolateral surface. In agreement with the results obtained by immunofluorescence experiments the GBS chimera was almost equally biotinylatable from both sides.

To perform functional studies, we first measured the kinetic parameters in the MDCK cell lines expressing wild type and mutated transporters. Similar apparent GABA affinity constants of about 30 μM were measured (data not shown), suggesting that GAT mutants retain the original GAT-1 GABA affinity. This result permitted measurements of functional activities in the apical or basolateral surface of wild type and mutants under the same experimental conditions (Fig. 5*C* and “Experimental Procedures”). GAT-1 and $\Delta\text{C-GAT}$ transfected-MDCK cells mediate a higher GABA influx at the apical *versus* the basolateral surface, whereas higher GABA influx was observed at the basolateral surface with BGT and myc BGT-transfected MDCK cells. Comparable apical and basolateral GABA influx levels were determined in GBS expressing MDCK cells. A comparison of the results obtained by biotinylation and GABA influx assays is presented in Fig. 5, *B* and *C*, respectively. The predominant apical localization of $\Delta\text{C-GAT}$ and the equal distribution in the apical and basolateral plasma membranes of GBS were confirmed by both methods. Thus, these data suggest the presence of a basolateral sorting signal in the cytosolic tail of BGT. However, this signal is not capable of completely reversing the polarity of GAT-1.

The Cytosolic Tail of BGT Is Sufficient to Redirect Basolaterally a Monotopic Protein—To investigate whether the identified basolateral signal of BGT is functional when transferred to a monotopic protein, we replaced the last COOH-terminal

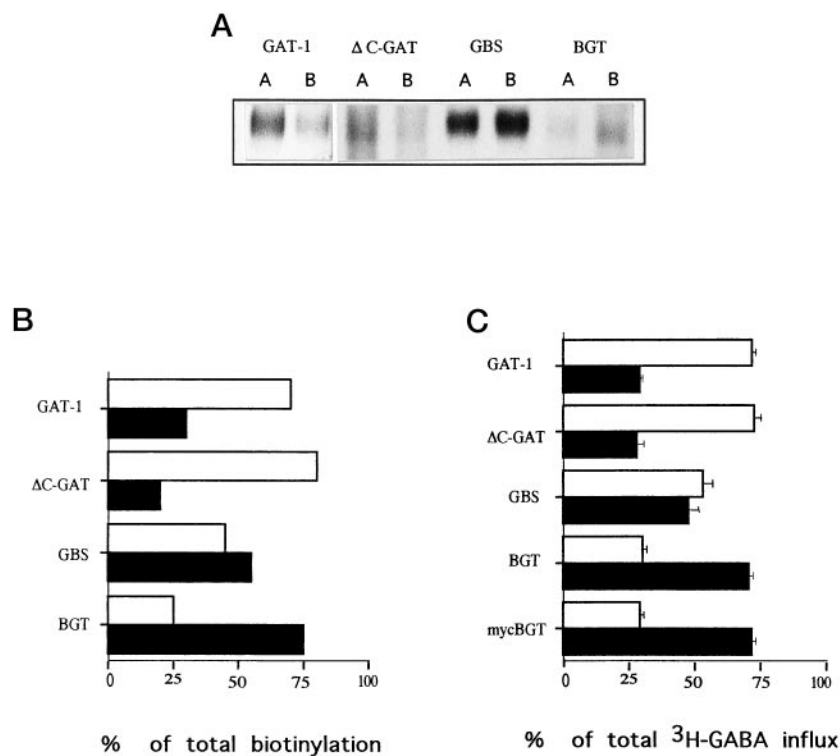


FIG. 5. Quantitation by surface biotinylation and GABA uptake assay of cell surface distribution of wild type and mutated GABA and betaine transporters expressed in MDCK cells. *Panel A*, steady-state biotinylation experiments were carried out in confluent transfected cells grown on Transwell filters. Cells were metabolically labeled overnight with [³⁵S]methionine and cysteine. Surface-expressed transporters were biotinylated from the apical (*A*) or basolateral (*B*) side. After cell lysis, the proteins were immunoprecipitated and then reprecipitated with streptavidin beads. The precipitates were analyzed on 10% SDS-polyacrylamide gel electrophoresis and visualized by fluorography. *Panel B*, quantification of apical and basolateral surface expression of transporters assayed by cell surface biotinylation. Densitometric quantitation of the biotinylation experiment shown in *panel A* is presented as the percent of total cell surface (apical + basolateral) biotinylated transporters. *Panel C*, quantification of apical and basolateral transporter activity assayed by [³H]GABA uptake. [³H]GABA influx measurements were carried out on cells grown confluent in Transwell filters at a final [³H]GABA concentration of 10 μM for wild type and GAT-1 mutants and of 100 μM for BGT-related transporters. Labeled GABA was applied from the apical or basolateral surface and the total activity measured was: ~35 (GAT-1), 16 (ΔC-GAT), 20 (GBS), 7 (BGT), and 5.5 (myc BGT) pmol/min/well. Values are presented as the percent of total cell surface transporter activity and represent means ± S.E. of at least five independent experiments performed in duplicate. *Empty and filled columns* indicate apical and basolateral surfaces, respectively. *Bars* indicate S.E.

150 amino acid residues of p75 hNGFR with the 51 amino acids of the BGT tail (hNGFR-BGT chimera). P75 hNGFR is a type I transmembrane glycoprotein that has been shown elsewhere (4) to localize apically when transfected in MDCK cells. It has also been shown that the apical distribution persists after deletion of the cytoplasmic domain (XI mutant) and that an internal deletion within the cytosolic domain (PS mutant), which creates a basolateral sorting signal, is able to redirect the receptor basolaterally. Because of this sorting behavior, hNGFR appears to be suitable as polarity reporter protein. Wild type and hNGFR-BGT chimera were transfected into MDCK cells and their distribution detected by immunofluorescence and cell surface immunoprecipitation of biotinylated receptors using mAb ME 20.4. The apical distribution of hNGFR revealed in vertical and horizontal sections, obtained by confocal analysis, is shown in Fig. 6, *a* and *b*, respectively. The BGT tail relocated basolaterally the apical hNGFR (Fig. 6, *c* and *d*). These experiments were carried out in nonpermeabilized cells to avoid the interference in surface receptor detection due to the high intracellular expression of both wild type and chimeric receptor. Cell surface biotinylation experiments carried out in MDCK-transfected cells confirmed the predominant basolateral localization of the hNGFR-BGT chimera (Fig. 6*B*).

An 8-Amino Acid Region within the Cytoplasmic Tail of BGT Contains Information Necessary for the ER Exit of BGT and for the Basolateral Localization of the GBS Chimera—A comparison of the amino acid sequences of the cytosolic tails of BGT (dog and human) and GAT-1 reveals a region, proximal to the

plasma membrane, which is rich in positively charged amino acids and conserved in the BGT sequence of dog and man but not in the GAT-1 sequence (Fig. 7*A*). Since a similar sequence is a basolateral sequence for the poly IgR (8) we deleted this region in both the wild type BGT and GBS chimera (BGT and GBS Δ 565–572, respectively), and their cellular distribution was analyzed by indirect immunofluorescence microscopy and [³H]GABA influx studies. Confocal images revealed an intracellular accumulation of the BGT Δ 565–572 construct (Fig. 7*B*), and influx studies confirmed the absence of surface localization of the mutant transporter (data not shown). In contrast to the results obtained with the BGT Δ 565–572, the deleted GBS chimera (GBS Δ 565–572) was able to reach the cell surface and, more interestingly, the deletion restored the original apical localization of GAT-1 (Fig. 7*B*). Influx experiments performed on several GBS Δ 565–572 MDCK-transfected cell lines confirmed the predominant apical localization of the deleted GBS chimera (see in Fig. 7*C* the comparison of the average uptake of several clones expressing the deleted GBS chimera with GAT and GBS). Thus, our data indicate that information necessary for both the BGT export from the ER and for the basolateral localization of the GBS chimera is contained within amino acids 565–572 of BGT.

DISCUSSION

The presence of three distinct domains has made monotopic proteins useful models with which to identify the sequences

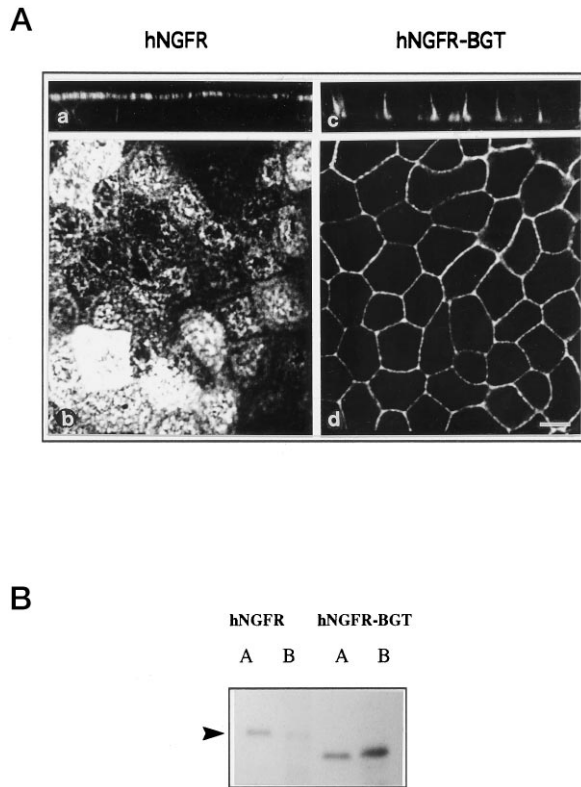


FIG. 6. Surface distribution of the wild type hNGFR and hNGFR-BGT chimera. Panel A, indirect immunofluorescence analysis. Confluent monolayers expressing wild type hNGFR (a and b) or chimeric receptor hNGFR-BGT (c and d) were grown on Transwell filters and fixed with 3% paraformaldehyde. The cells were then incubated in the absence of detergent with mouse anti-hNGFR (ME 20.4) antibody. Vertical (a and c) and horizontal (b and d) sections were taken by confocal microscopy. Bar, 10 μ m. Panel B, cell surface biotinylation was performed as described in the legend for Fig. 5A, and anti-hNGFR mAb 20.4 antibody was used to immunoprecipitate the wild type and chimeric receptor. Densitometric quantitation of the cell surface biotinylation experiments indicated that the BGT tail relocated basolaterally 75% of the hNGFR. The position corresponding to the apparent molecular weight of the hNGFR is indicated on the left by an arrowhead.

responsible for apical and basolateral sorting in polarized cells. Indeed, studies with truncated and chimeric monotopic proteins have led to the conclusion that basolateral sorting signals are contained in the cytosolic domain of basolaterally located proteins whereas apical sorting signals are probably contained in the luminal/transmembrane domains of apical proteins (2).

To perform the characteristic transepithelial transport of solutes and water, polarized epithelia must sort distinct classes of transporter proteins selectively to their apical or basolateral surfaces. Transport proteins are polytopic proteins consisting of several cytosolic and luminal/transmembrane domains. Their sorting has thus proven difficult and complex to analyze. In spite of the complexity of the system it is of particular interest to understand if polytopic proteins follow the same rules established for monotopic proteins.

So far, the sorting behavior of polytopic proteins has been investigated principally using as models two proteins belonging to the E1-E2 class of ion-transporting ATPases, the α 1 subunits of the Na,K- and the H,K-ATPases. From these studies, an apical sorting signal was found to be contained within the amino-terminal half of the H,K-ATPase (16). More recently this signal has been located to 8 amino acids in the 4th trans-

membrane domain.² From these results, it would appear that the apical signals of polytopic proteins might be located in the luminal/transmembrane domains just as they are in monotopic proteins. A recent report indicates that the basolateral localization of the Na,K-ATPase, rather than being mediated by a basolateral sorting signal, might derive both from its exclusion from the apical pathway and from a cytoskeleton-mediated retention mechanism operating selectively on the basolateral plasma membrane (35). Moreover, in contrast with the behavior documented for several membrane proteins, which maintain a polarized distribution in both MDCK cells and hippocampal neurons (36, 37), two isoforms of the Na,K-ATPase with exclusive basolateral localization in MDCK cells are distributed homogeneously in neuronal (hippocampal) cells (26). Our observations of a nonpolarized neuronal expression *versus* the exclusive epithelial basolateral localization of the sodium pump taken together with the report of Mays *et al.* (35) might lead to the conclusion that polytopic proteins make use of different sorting mechanisms than monotopic proteins to localize basolaterally.

BGT and GAT-1 are homologous polytopic proteins that exhibit opposite sorting behavior in both neuronal and epithelial cells (1, 38). We have used these two proteins as models to compare the sorting mechanisms of mono- and polytopic proteins. In particular, in this study we have investigated the role of the cytosolic COOH-terminal domains of GAT-1 and BGT.

Distinct Roles of the Carboxyl Termini of GAT-1 and BGT—Our data on the truncated GABA transporter (Δ C-GAT) demonstrate that the cytoplasmic COOH-terminal domain of GAT-1 is not necessary either for its apical sorting or for its functional activity. The latter observation is in agreement with a previous *in vitro* study of Mabjeesh and Kanner (39). The authors showed that a proteolytic fragment of purified GAT-1 lacking the cytosolic and most likely the last transmembrane domain still exhibits transport activity upon reconstitution in liposomes. Our results demonstrate that 36 amino acids at the carboxyl terminus of GAT-1 are not required for GABA transport and, furthermore, to localize the transporter on the apical plasma membrane of MDCK cells.

Because of the structural similarity of BGT with the GAT-1, the ER localization of Δ C-myc BGT was not expected. Moreover, both a short deletion in the BGT tail (BGT Δ 565–572) as well as the tail replacement with that of GAT-1 (BGS chimera) generates transporters that fail to reach the cell surface. Many natural and artificial mutations have been observed to result in ER retention and degradation, apparently because they affect protein folding or oligomerization (40). So far, studies on the oligomerization of GABA and betaine transporters have not been carried out, but an oligomeric structure has been inferred for several carrier systems, and an oligomeric structure has been documented in the case of the glucose transporter (41) and Na/H exchanger (42). Our data suggest a direct involvement of an 8-amino acid region in the COOH terminus of BGT in the folding/oligomerization process of the betaine transporter. Further investigations are required to clarify the cellular process in which this sequence is involved. However, the present work provides clear evidence for a different role of the COOH-terminal domains of these two homologous proteins.

Comparison between Sorting Signals of Monotopic and Polytopic Proteins—We have identified a basolateral sorting signal contained in the cytosolic tail of BGT. This signal is functional when transferred on otherwise apically located proteins and presents similarities with those identified in monotopic proteins, since it is located in a cytosolic domain. Our data with the

² M. J. Caplan, unpublished data.

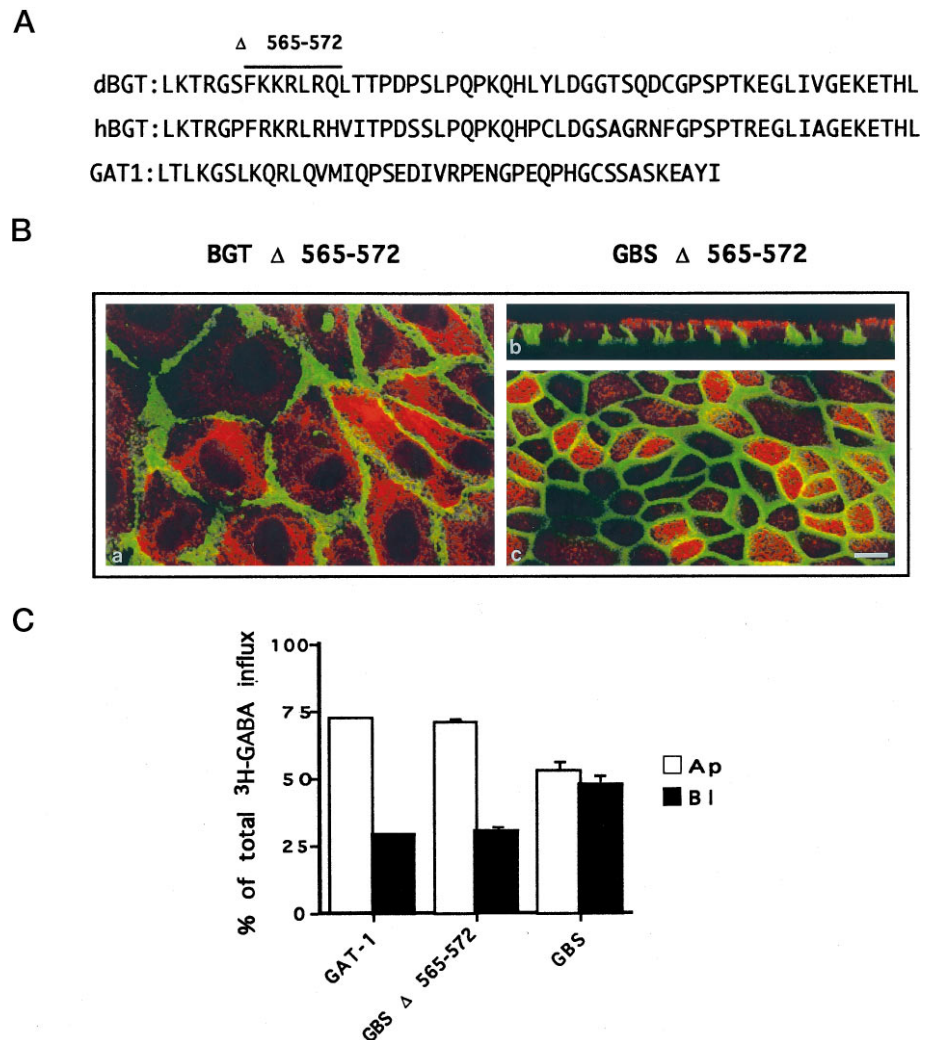


FIG. 7. Distribution of BGT Δ565-572 and GBS Δ565-572 expressed in MDCK cells. *Panel A*, comparison between the cytosolic tails of canine and human BGT and of rat GAT-1. The region containing amino acids 565-572 of BGT, deleted from BGT and GBS cDNAs, is indicated. *Panel B*, immunofluorescence analysis of MDCK transfected with BGT Δ 565-572 (*a*) or GBS Δ 565-572 (*b* and *c*), stained with antibodies BGT-KLH (in red) and mAb 6H against the sodium pump (in green). Merging of horizontal (*a*) and vertical (*b* and *c*) confocal sections is shown. In *a* the enlarged shape of the cells is due to the overnight treatment with sodium butyrate. *Bar*, 15 μm. *Panel C*, quantification of apical (empty columns) and basolateral (filled columns) transport activity assayed by [³H]GABA uptake. Values are presented as the percent of total cell surface transporter activity and represent means ± S.E. of five independent GBS Δ 565-572 expressing cell lines performed in duplicate. The comparison of the apical to basolateral ratio between GBS Δ 565-572, wild type GAT-1, and GBS constructs together with the immunofluorescence experiments indicates that a basolateral signal is contained in the 8-amino acid deleted region within the cytosolic tail of BGT. Moreover, this region contains information necessary for the ER exit of BGT.

hNGFR-BGT and GBS chimeras demonstrate that this signal can redirect both a monotopic (the hNGFR) and a polytopic (the GAT-1) protein, normally located on the apical surface, to the basolateral surface of MDCK cells. We have mapped to an 8-amino acid region the information necessary to localize basolaterally the GBS chimera. In fact, a deleted GBS chimera that lacks 8 residues but retains the rest of the BGT tail (GBS Δ 565-572) was sorted apically. The 8-amino acid region is rich in basic residues and, interestingly, basic residues have been shown to play a role in the basolateral sorting of monotopic proteins (4, 5, 43). In case of the poly IgR, basolateral sorting seems to depend, as shown by alanine scanning mutagenesis, on a 3-basic residue segment. Further analysis is required to determine the contribution of the positively charged residues for the basolateral sorting of GBS and BGT. Unfortunately, the inability of both the tail-minus and the Δ565-572 BGT to move out of the ER prevented us from directly testing the role of the entire cytosolic tail and of the 8-amino acid region in the basolateral sorting of the transporter. Most of the basolateral sorting signals so far identified rely on a tyrosine residue (2). Since the tyrosine residue in the canine BGT tail is not conserved in the human BGT homolog (44), a prevalent role of the tyrosine residue in the basolateral sorting of BGT seems unlikely, although it remains to be investigated.

Although the basolateral sorting signal contained in the BGT tail which we identify completely reverses the apical localization of the monotopic hNGFR (hNGFR-BGT chimera) it only partially relocates the polytopic GAT-1 (GBS chimera). Since

the signal contained in the BGT tail is dominant on the apical sorting signal of the hNGFR we exclude the presence in the BGT tail of a weak basolateral signal while we favor the explanation of both apical and basolateral sorting signals of comparable strength in the GBS chimera. This explanation implies that apical sorting signals of this polytopic protein might not be recessive to basolateral sorting signals, in contrast to the results obtained with monotopic proteins (2). In a recent report Turner *et al.* (17) showed that the basolateral sorting sequence from a monotopic protein can direct basolaterally a polytopic apical protein in Caco-2 cells. The authors have epitope tagged the sodium-dependent glucose cotransporter (SGLT1) with the sequence containing the residues most relevant to determine basolateral sorting of the vesicular stomatitis virus G protein. Similarly to our GBS chimera results, the tagged SGLT1 localized contemporaneously in both the apical and basolateral surfaces. Thus, our results and those on the SGLT1 taken together indicate that basolateral sorting signals can be exchangeable between mono- and polytopic proteins, but they might behave as dominant only when introduced in monotopic proteins.

In conclusion, our results suggest that similar mechanisms may underlie the sorting of polytopic and monotopic proteins in polarized epithelial cells. There are also, however, important differences, such as in the apparent strength of apical sorting signals. The future study of the sorting mechanisms of this type of protein may thus yield novel information on the genesis of epithelial polarity.

Acknowledgments—We thank Drs. B. Kanner, J. Handler, A. Le Bivic, R. Jahn, and D. Louvard for providing reagents. We also thank Dr. F. Clementi and the members of the Borgese/Fornasari laboratories for helpful suggestions and reading of the manuscript. Special thanks go to Drs. F. Clementi and N. Borgese for support and encouragement.

REFERENCES

- Pietrini, G., Suh, Y. J., Edelmann, L., Rudnick, G., and Caplan, M. J. (1994) *J. Biol. Chem.* **269**, 4668–4674
- Matter, K., and Mellman, I. (1994) *Curr. Opin. Cell Biol.* **6**, 545–554
- Brewer, C. B., and Roth, M. G. (1991) *J. Cell Biol.* **114**, 413–421
- Le Bivic, A., Sambuy, Y., Patzak, A., Patil, N., Chao, M., and Rodriguez-Boulan, E. (1991) *J. Cell Biol.* **115**, 607–618
- Matter, K., Hunziker, W., and Mellman, I. (1992) *Cell* **71**, 741–753
- Geffen, I., Fuhrer, C., Leitinger, B., Weiss, M., Huggel, K., Griffiths, G., and Spiess, M. (1993) *J. Biol. Chem.* **268**, 20772–20777
- Thomas, D. C., Brewer, C. B., and Roth, M. G. (1993) *J. Biol. Chem.* **268**, 3313–3320
- Casanova, J. E., Apodaca, G., and Mostov, K. E. (1991) *Cell* **66**, 65–75
- Dargement, C., Le Bivic, A., Rothenberger, S., Iacopetta, B., and Kuehn, L. C. (1993) *EMBO J.* **12**, 1713–1721
- Lisanti, M. P., Sargiacomo, M., Graeve, L., Saltiel, A., and Rodriguez-Boulan, E. (1988) *Proc. Natl. Acad. Sci. U. S. A.* **85**, 9557–9561
- Rodriguez-Boulan, E., and Powell, S. K. (1992) *Annu. Rev. Cell. Biol.* **8**, 395–427
- Brown, D. A., Crise, B., and Rose, J. K. (1989) *Science* **245**, 1499–1501
- Lisanti, M. P., and Rodriguez-Boulan, E. (1990) *Trends Biochem. Sci.* **15**, 113–118
- Scheiffele, P., Peranen, J., and Simons, K. (1995) *Nature* **378**, 96–98
- Prill, V., Lehmann, L., Von Figura, K., and Peters, C. (1993) *EMBO J.* **12**, 2181–2193
- Gottardi, C. J., and Caplan, M. J. (1993) *J. Cell Biol.* **121**, 283–293
- Turner, J. R., Lencer, W. I., Carlson, S., and Madara, J. L. (1996) *J. Biol. Chem.* **271**, 7738–7744
- Guastella, J., Nelson, N., Nelson, H., Czyzyk, L., Keynan, S., Miedel, M. C., Davidson, N., Lester, H. A., and Kanner, B. I. (1990) *Science* **249**, 1303–1306
- Yamauchi, A., Uchida, S., Kwon, H. M., Preston, A. S., Robey, R. B., Garcia-Perez, A., Burg, M. B., and Handler, J. S. (1992) *J. Biol. Chem.* **267**, 649–652
- Amara, S. G., and Arriza, J. L. (1993) *Curr. Opin. Neurobiol.* **3**, 337–344
- Radian, R., Ottersen, O. P., Storm-Mathisen, J., Castel, M., and Kanner, B. I. (1990) *J. Neurosci.* **10**, 1319–1330
- Yamauchi, A., Kwon, H. M., Uchida, S., Preston, A. S., and Handler, J. S. (1991) *Am. J. Physiol.* **261**, F197–F202
- Hempstead, B. L., Patil, N., Thiel, B., and Chao, M. V. (1990) *J. Biol. Chem.* **265**, 9595–9598
- Liu, F. T., Zinnecker, M., Hamaoka, T., and Katz, D. H. (1979) *Biochemistry* **18**, 690–697
- Gotti, C., Moretti, M., Longhi, R., Briscini, L., Manera, E., and Clementi, F. (1993) *J. Recept. Res.* **13**, 453–465
- Pietrini, G., Matteoli, M., Banker, G., and Caplan, M. J. (1992) *Proc. Natl. Acad. Sci. U. S. A.* **89**, 8414–8418
- Monlauzeur, L., Rajasekaran, A., Chao, M., Rodriguez-Boulan, E., and Le Bivic, A. (1995) *J. Biol. Chem.* **270**, 12219–12225
- Louvard, D., Reggio, H., and Warren, G. (1982) *J. Cell Biol.* **92**, 92–107
- Cameron, P. L., Sudhof, T. C., Jahn, R., and De Camilli, P. (1991) *J. Cell Biol.* **115**, 151–164
- Lisanti, M. P., Le Bivic, A., Sargiacomo, M., and Rodriguez-Boulan, E. (1989) *J. Cell Biol.* **109**, 2117–2127
- Sargiacomo, M., Lisanti, M., Graeve, L., Le Bivic, A., and Rodriguez-Boulan, E. (1989) *J. Membr. Biol.* **107**, 277–286
- Laemmli, U. K. (1970) *Nature* **227**, 680–685
- Matter, K., Yamamoto, E. M., and Mellman, I. (1994) *J. Cell Biol.* **126**, 991–1004
- Jackson, M. R., Nilsson, T., and Peterson, P. A. (1990) *EMBO J.* **9**, 3153–3162
- Mays, R. W., Siemers, K. A., Fritz, B. A., Lowe, A. W., van Meer, G., and Nelson, W. J. (1995) *J. Cell Biol.* **130**, 1105–1115
- Dotti, C. G., and Simons, K. (1990) *Cell* **62**, 63–72
- Dotti, C. G., Parton, R. G., and Simons, K. (1991) *Nature* **349**, 158–161
- Ahn, J., Mundigl, O., Muth, T. R., Rudnick, G., and Caplan, M. J. (1996) *J. Biol. Chem.* **271**, 6917–6924
- Mabjeesh, N. J., and Kanner, B. I. (1992) *J. Biol. Chem.* **267**, 2563–2568
- Klausner, R. D., and Sitia, R. (1990) *Cell* **62**, 611–614
- Stevens, B. R., Fernandez, A., Hirayama, B., Wright, E. M., and Kemper, E. S. (1990) *Proc. Natl. Acad. Sci. U. S. A.* **87**, 1456–1460
- Fafournoux, P., Noel, J., and Pouyssegur, J. (1994) *J. Biol. Chem.* **269**, 2589–2596
- Aroeti, B., Kosen, P. A., Kuntz, I. D., Cohen, F. E., and Mostov, K. E. (1993) *J. Cell Biol.* **123**, 1149–1160
- Rasola, A., Galiotta, L. J. V., Barone, V., Romeo, G., and Bagnasco, S. (1995) *FEBS Lett.* **373**, 229–233

Sorting of Two Polytopic Proteins, the γ -Aminobutyric Acid and Betaine Transporters, in Polarized Epithelial Cells

Carla Perego, Alessandra Bulbarelli, Renato Longhi, Marco Caimi, Antonello Villa, Michael J. Caplan and Grazia Pietrini

J. Biol. Chem. 1997, 272:6584-6592.
doi: 10.1074/jbc.272.10.6584

Access the most updated version of this article at <http://www.jbc.org/content/272/10/6584>

Alerts:

- [When this article is cited](#)
- [When a correction for this article is posted](#)

[Click here](#) to choose from all of JBC's e-mail alerts

This article cites 44 references, 25 of which can be accessed free at <http://www.jbc.org/content/272/10/6584.full.html#ref-list-1>